SANDIA REPORT
SAND2001-3517
Unlimited Release
Printed November 2001

Interpreting Fracture Patterns in Sandstones Interbedded with Ductile Strata at the Salt Valley Anticline, Arches National Park, Utah

John C. Lorenz and Scott P. Cooper

Prepared by
Sandia National Laboratories
Albuquerque, New Mexico 87185 and Livermore, California 94550

Sandia is a multiprogram laboratory operated by Sandia Corporation, a Lockheed Martin Company, for the United States Department of Energy under Contract DE-AC04-94AL85000.

Issued by Sandia National Laboratories, operated for the United States Department of Energy by Sandia Corporation.

Available to DOE and DOE contractors from
U.S. Department of Energy
Office of Scientific and Technical Information
P.O. Box 62
Oak Ridge, TN 37831

Telephone: (865)576-8401
Facsimile: (865)576-5728
E-Mail: reports@adonis.osti.gov
Online ordering: http://www.doe.gov/bridge

Available to the public from
U.S. Department of Commerce
National Technical Information Service
5285 Port Royal Rd
Springfield, VA 22161

Telephone: (800)553-6847
Facsimile: (703)605-6900
E-Mail: orders@ntis.fedworld.gov
Online order: http://www.ntis.gov/ordering.htm

SAND2001-3517
Unlimited Release
Printed November 2001

Interpreting Fracture Patterns in Sandstones Interbedded with Ductile Strata at the Salt Valley Anticline, Arches National Park, Utah

John C. Lorenz and Scott P. Cooper
Geophysical Technology Department
Sandia National Laboratories
P.O. Box 5800
Albuquerque, NM 87185-0750

Abstract

Sandstones that overlie or that are interbedded with evaporitic or other ductile strata commonly contain numerous localized domains of fractures, each covering an area of a few square miles. Fractures within the Entrada Sandstone at the Salt Valley Anticline are associated with salt mobility within the underlying Paradox Formation. The fracture relationships observed at Salt Valley (along with examples from Paleozoic strata at the southern edge of the Holbrook basin in northeastern Arizona, and sandstones of the Frontier Formation along the western edge of the Green River basin in southwestern Wyoming), show that although each fracture domain may contain consistently oriented fractures, the orientations and patterns of the fractures vary considerably from domain to domain. Most of the fracture patterns in the brittle sandstones are related to local stresses created by subtle, irregular flexures resulting from mobility of the associated, interbedded ductile strata (halite or shale).

Sequential episodes of evaporite dissolution and/or mobility in different directions can result in multiple, superimposed fracture sets in the associated sandstones. Multiple sets of superimposed fractures create reservoir-quality fracture interconnectivity within restricted localities of a formation. However, it is difficult to predict the orientations and characteristics of this type of fracturing in the subsurface. This is primarily because the orientations and characteristics of these fractures typically have little relationship to the regional tectonic stresses that might be used to predict fracture characteristics prior to drilling. Nevertheless, the high probability of numerous, intersecting fractures in such settings attests to the importance of determining fracture orientations in these types of fractured reservoirs.

Table of Contents

1.0 Introduction……..……6

2.0 Salt Valley Anticline, Utah ……7
2.1 Introduction and Geologic Setting ……7
2.2 Fracture Patterns in the Entrada Formation of the Salt Valley Anticline ……..12
2.2.1 Fracture Domain A ……..14
2.2.2 Fracture Domain B ……...16
2.2.3 Fracture Domain C ……..……19
2.2.4 Fracture Domain D ……...……22
2.2.5 Fracture Domain E ……...25
2.2.6 Fracture Domain F ……...……25
2.2.7 Fracture Domain G ……..31
2.2.8 Fracture Domain H ……..31
2.3 Applicability: Cane Creek Shale ……31

3.0 Holbrook Anticline, Eastern Arizona ……..……...33

4.0 Frontier Formation, Hogsback Thrust Plate, Southwestern Wyoming ……..39

5.0 Conclusions ……..……..44

6.0 Acknowledgements ……..……44

7.0 References ……45

List of Figures

Figure 1: Location map for Arches National Monument ……..……..8
Figure 2: Aerial photograph of Salt Valley Anticline ……..……9
Figure 3: Cross-section of Salt Valley Anticline ……..10
Figure 4: Stratigraphic column for Arches National Park ……11
Figure 5: Structure and fracture map of the northeastern limb of Salt Valley Anticline …...…...13
Figure 6: Aerial photograph and sequence of fracture development for Fracture Domain A .15, 16
Figure 7: Aerial photograph and sequence of fracture development for Fracture Domain B .17, 18
Figure 8: Aerial photograph of Fracture Domain C ……..……..…..20
Figure 9: Sequence of fracture development for Fracture Domain C ……..……21
Figure 10: Aerial photograph of Fracture Domain D ……..……..23, 24
Figure 11: Sequence of fracture development for Fracture Domain D ……25
Figure 12: Aerial photograph of Fracture Domain E ……..……..26
Figure 13: Aerial photograph of Fracture Domain E ……..……...27
Figure 14: Sequence of fracture development for Fracture Domain E ……28
Figure 15: Aerial photograph of Fracture Domain F ……...…….29
Figure 16: Sequence of fracture development for Fracture Domain F …..……...30

Figure 17: Aerial photograph of the Courthouse Syncline ……..……..32
Figure 18: Isopach map and cross-section of the Holbrook Anticline …….……..34
Figure 19: Aerial photograph of "The Sinks" ……35
Figure 20: Photographs of fractures at the Holbrook Anticline ……..…….36, 37
Figure 21: Aerial photograph of the Twin Lakes area, Holbrook Anticline ……..38
Figure 22: Structural trends and fracture patterns along the Hogsback Thrust …….40
Figure 23: Aerial photograph of fractures in a structurally simple area ……41
Figure 24: Aerial photograph of the changing strike of the Hogsback Thrust ……..42
Figure 25: Aerial photograph of oblique fracture patterns along the Hogsback Thrust ……43

1.0 INTRODUCTION

Relatively brittle reservoir strata such as sandstones are prone to fracture under stress. Most outcroppings of sandstone are fractured, and wherever definitive data exist, most subsurface sandstones are also known to be fractured to varying degrees. Both regional and local stresses are capable of creating such fractures. One way to create significant, local stresses in sandstones is to flex them by the addition or removal of material to the adjacent beds. For example, the ability of relatively ductile strata such as evaporites and certain types of shales to move laterally in the subsurface allows the formation of local but significant thicks and thins that flex the interbedded non-ductile strata. Additionally, dissolution of evaporites removes material locally, again flexing strata in order to accommodate the change in evaporite thickness at the dissolution front. Finally, wedges of heterogeneous material that are pushed laterally, as in a thrust plate, will be rearranged internally according to the variable material properties in the wedge, creating local stresses and related local fracture patterns.

Because the range of structural variability under such conditions is wide, and the constraints on parameters such as mechanical properties and timing of movements are poor, it is difficult to predict subsurface fracture patterns in such conditions prior to drilling. However, the fracture domains at Salt Valley do provide a suite of patterns that may be useful as analogies for similar subsurface reservoirs. This study provides insights into the range of possibilities for fracture patterns in such settings.

The spectacular and varied fractures found in the Mesozoic sandstones overlying mobile Paleozoic evaporites of the Paradox basin, as seen in outcrop at Arches National Park, southeastern Utah will be emphasized in this report and compared with additional field data from the following two sites:

1) The reactivated regional fractures found in the abruptly folded and extended Paleozoic Coconino sandstones that overlie a salt dissolution front at the southern edge of the Holbrook basin in eastern Arizona.
2) The sandstones of the Frontier Formation within the shaley Upper Cretaceous section, which has been incorporated into the Hogsback Thrust of the Sevier, Idaho-Wyoming thrust belt in southwestern Wyoming.

The well exposed, outcrop system at Arches National Monument provides a wealth of data that can be interpreted and characterized in three dimensions. However, this system and the two supporting systems would be difficult to characterize from a limited suite of downhole or geophysical measurements.

2.0 SALT VALLEY ANTICLINE, UTAH

2.1 Introduction and geologic setting

The Moab and Slickrock members of the Jurassic Entrada Formation have large, extensively fractured, bedding-plane exposures on the limbs of the Salt Valley anticline in Arches National Park, southeastern Utah (Figures 1, 2). The fracture patterns are regular and consistent at the sub-kilometer scale, yet are diverse at the scale of the over 40 km-long, NW-SE trending anticline. The Salt Valley anticline formed over an elongated, evaporite-cored diapiric structure (Figure 3) that has a compound history of salt mobility, beginning contemporaneously with or soon after deposition and continuing intermittently through to the present (e.g., Dyer, 1983; Doelling, 1985, 1988, 2000; Oviatt, 1988; Cruikshank and Aydin, 1995; Hudec and May, 1998, 1999). Evidence for this includes unconformities in the sedimentary record, thickness changes in sedimentary rock units and deformed Quaternary deposits. The evaporite core itself is over 3600m thick and composed of primarily halite (87%) with some potash. The remaining volume consists of anhydrite, dolomite and shale (Hite, 1977). Most of the fractures in the Entrada sandstones appear to be related to flexure of the strata during thinning and thickening due to lateral flow of salt within the Paradox Formation 1500 meters below the Entrada (Lorenz and Neal, 1997). This flow resulted in flexure and fracturing of the Entrada sandstones (Dyer, 1983), within rim synclines overlying areas of salt withdrawal and over anticlines above salt accumulations, and at local twists and compound curves.

The Entrada Sandstone and the conformably overlying Summerville Formation are part of the San Rafael Group (Figure 4; Dyer, 1983). The Entrada Sandstone is approximately 150 m thick and can be subdivided in ascending order into the Dewey Bridge Member, the Slick Rock Member and the Moab Member. The Dewey Bridge Member varies in thickness from 6m to greater than 30 m. This member is an orange to orange/red unit of interbedded siltstones, mudstones, and sandstones, possibly representing a lagoonal depositional environment. The Slick Rock Member is a 1-5 m thick, orange to dark red, massive, fine-grained sandstone deposited in a near shore to shallow marine environment. The Moab Member, containing most of the fractures described within this report, is a light-gray to white, 27 m thick, medium to fine-grained sandstone representing a near shore beach and dune environment.

The Entrada Formation delineates the surface expression of the Salt Valley anticline. Removal of overlying shales has left the upper bedding surface of the Entrada exposed over large areas, and the topographic contours of this pavement provide a natural structure-contour map over much of the anticline. These contours document the subtly twisted and folded nature of this unit, and allow insights into the relationship between the anticline, the mobility of the underlying salt, and the associated fractures.

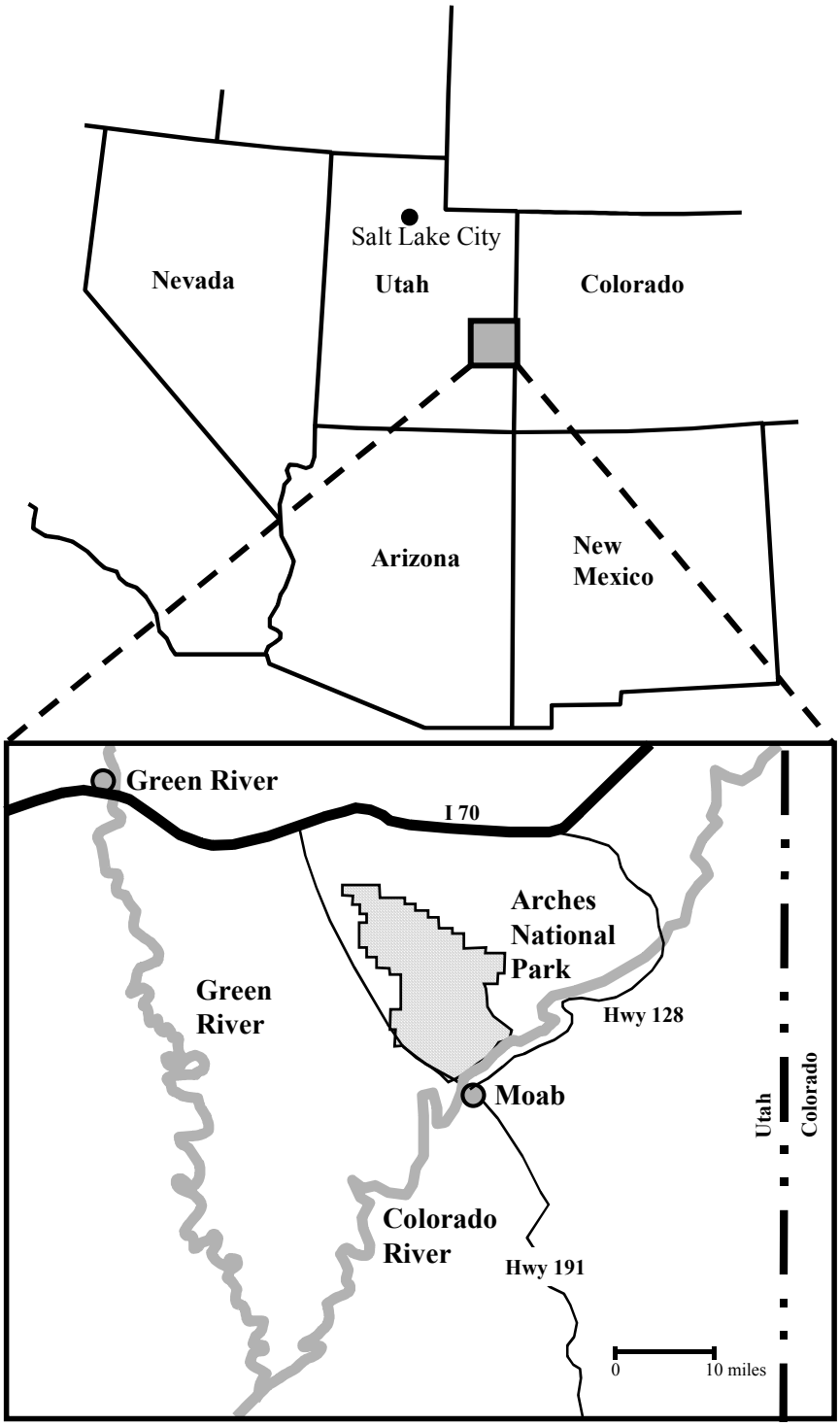

Figure 1: Arches National Monument is located directly north of Moab in southeastern Utah.

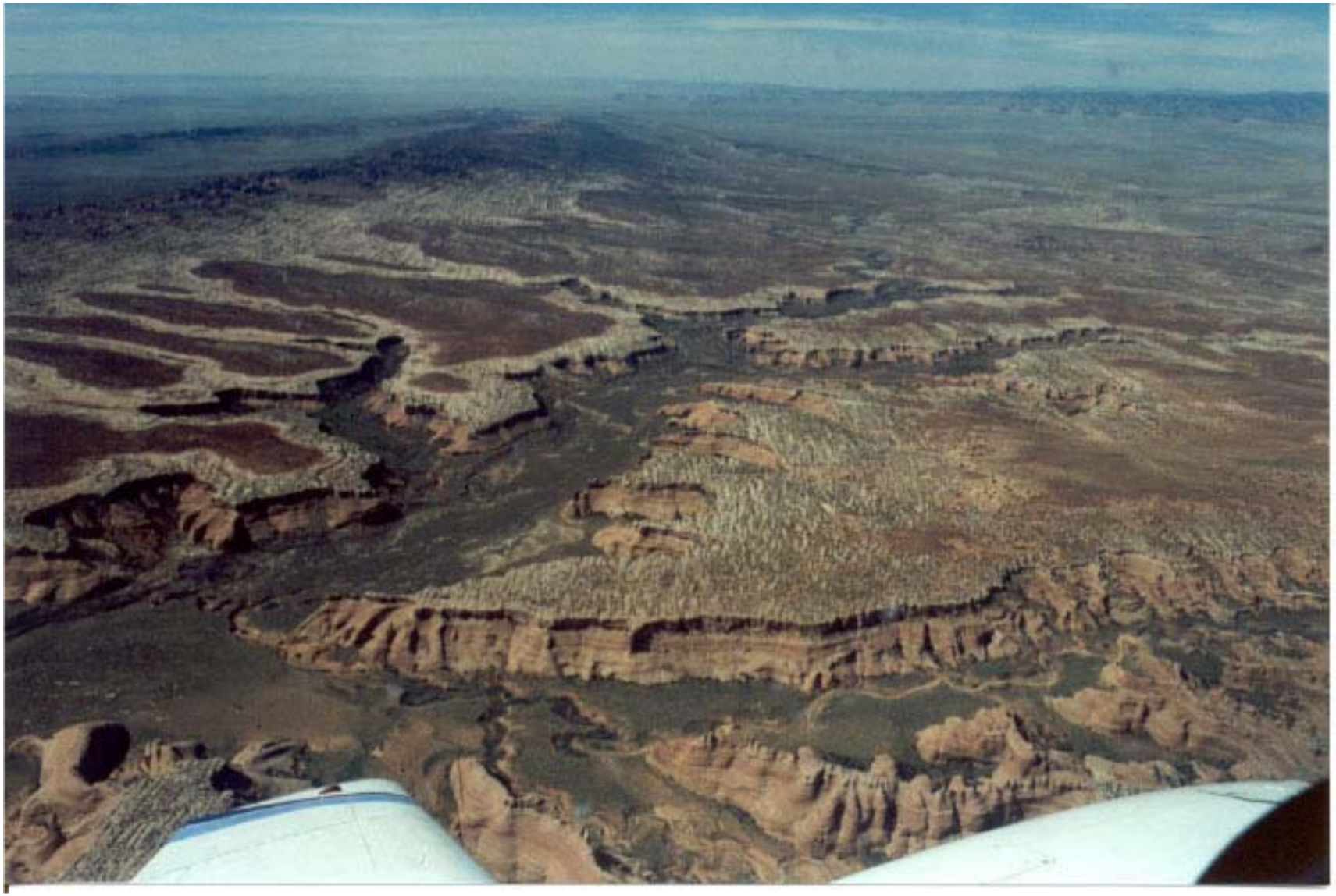

Figure 2: View is northwestward along the northeast limb of the breached, salt-cored Salt Valley Anticline. Numerous fractures can be seen in this aerial photograph as a "texture" on the white caprock, which is the Slickrock Member of the Entrada Formation.

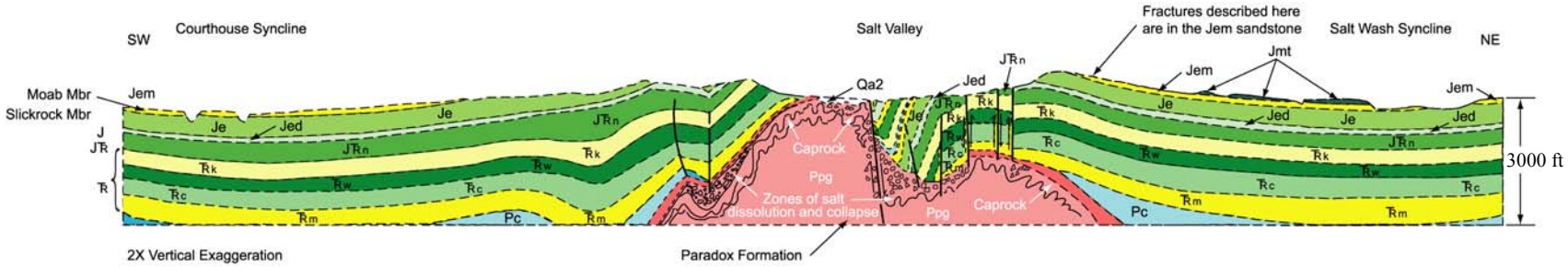

Figure 3: Cross-section of the Salt Valley Anticline illustrating the evaporitic-core of this diapiric structure (from Doelling, 1985). Jmt = Tidwell Member of the Morrison Formation; Jem = Moab Tongue of the Entrada Sandstone; Je = Slickrock Member of the Entrada Sandstone; Jed = Dewey Bridge Member of the Entrada Sandstone; JTRn = Navajo Sandstone; TRk = Kayenta Formation; TRw = Wingate Sandstone; TRc = Chinle Formation; TRm = Moenkopi Formation; Pc = Cutler Formation; Ppg = Paradox Formation.

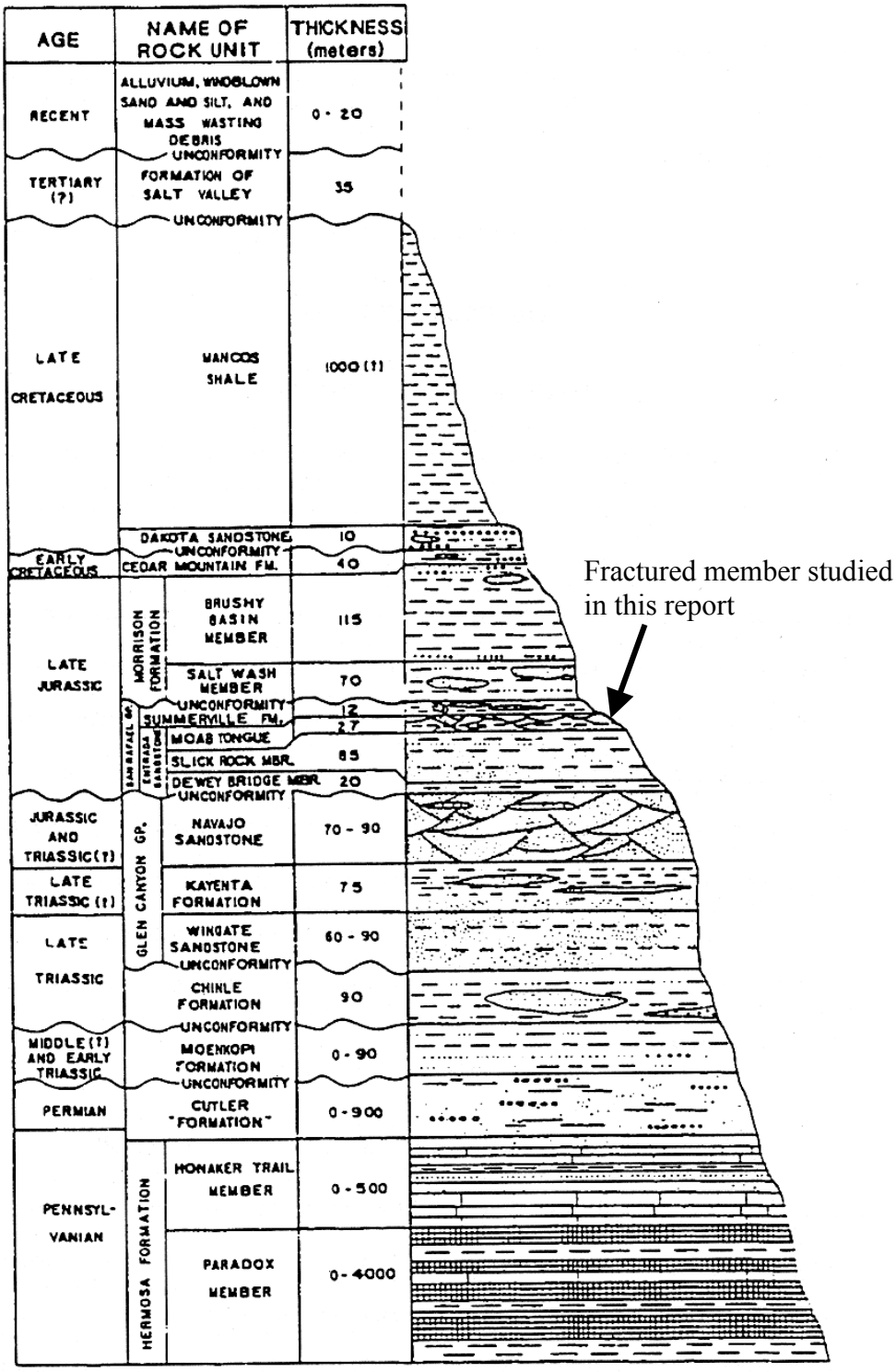

Figure 4: Generalized stratigraphic column for the Arches National Park region (from Dyer, 1983)

2.2 Fracture Patterns in the Entrada Formation of the Salt Valley Anticline

In their most generalized form, fractures in the Entrada Formation trend sub-parallel to the long axis of the anticline, reflecting arching and stretching of the strata normal to the long axis of a rising pillow of salt. However, some of the fracture patterns are not directly related to the present structural configuration because of the compound history of the structure, and the earlier history of the flexures caused by now-obscure salt migration must be postulated and reconstructed from the preserved record of the fractures in these areas. Some fracture sets may be related to earlier episodes and directions of evaporite mobility and thus are not geometrically related to the present-day structure. Superimposed fracture sets may also have been created during successive mobility events. The flexure that caused many of the fracture patterns cannot be reconstructed due to obscuration of the evidence by later events.

Fractures observed from a distance at Arches National Park are typically composed of zones of smaller-scale fractures (Dyer, 1983; Cruikshank and Aydin, 1995). Many of these natural fracture zones on the Salt Valley Anticline have been weathered and filled in with vegetation and wind-blown sand. Therefore, large-scale fracture-pattern signatures are more readily studied from a distance than when standing directly on the outcrop. High-altitude air photos provided the initial basis for the pattern recognition and characterization presented here. These photos were supplemented with low-altitude, oblique aerial photography that provided more detail of the structure-fracture relationships.

The fractures in sandstones at Arches National Park have been intensively studied by previous authors (e.g., Dyer, 1983, 1988; Doelling, 1988; Zhao and Johnson, 1991, 1992; Cruikshank and Aydin, 1994, 1995), primarily on the southwestern limb of the Salt Valley Anticline. The focus of most of these previous studies has been on interpreting the interactions between different fracture sets at the outcrop scale. Few of the authors have tried to relate fracture origins to regional or local stresses. However, they have provided an important background for this study, which approaches the problem at a larger scale, relating the fracture patterns to the stresses created by the subtle structures and structural history of the area. Meter-scale characteristics such as individual fracture interactions or the fractography of fracture surfaces are not addressed here. This study concentrated on the northeastern limb of the anticline where the fracture-structure relationships are relatively clear cut. The fracture domains and areas studied in this report are different from the areas previously studied by the aforementioned authors. However, the systems of fractures observed are similar. Kilometer-scale fracture domains can be readily identified and these domains are related to lithology and salt movement in the underlying Paradox Formation.

A map of the structure of the northeastern limb of the Salt Valley Anticline with the superimposed natural fracture patterns shows seven fracture domains (A-G, Figure 5), with transitional areas between them. Most of these domains can be interpreted in terms of the twisting and flexure of the beds, although the fracture-structure relationships are obscure in some areas due to the cumulative history of different stages of salt mobility and local changes in the structure after fracturing.

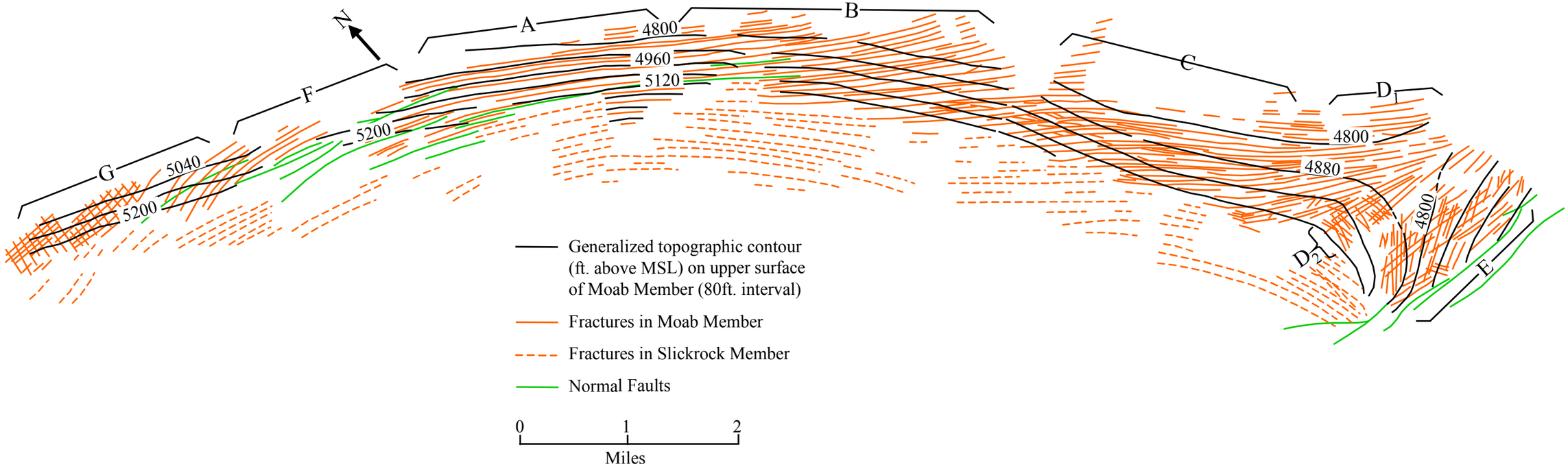

Figure 5: Structure map of the northeastern limb of the Salt Valley Anticline with the natural fracture patterns superimposed, illustrating seven fracture domains and the transition zones between the domains.

2.2.1 Fracture Domain A

Arching of the Entrada sandstones over the rising salt core of the anticline caused extension fractures to form, striking parallel to the axis of the arch and normal to the axis of maximum extension (Figures 5, 6A,B). In fact, several normal faults have been mapped in this area (Doelling, 1985), striking parallel to the structural and fracture strikes and indicating that extensile strain exceeded that required for fracturing, probably exploiting fracture-provided planes of weakness. This basic, 'primitive' fracture pattern of parallelism between fracture strike and bedding strike is preserved in the five-square-kilometer area of domain A (Figure 6A). Growth of the anticline, both in height and length, and the coalescence of smaller features to form the present structure, has complicated this fracture-structure relationship on other parts of the structure.

The present northeasterly dip in this area averages about 8^{o}, although the strata on the limb are slightly concave-upward (by about 20 m of deflection from the straight-line dip across 1 km). This suggests that uplift did not increase at a uniform rate towards the anticlinal crest (i.e., that diapiric uplift became concentrated along the crest during the late stages of development), and shows that the fractured strata were not uplifted as a planar slab. Evaporitic strata were withdrawn from beneath the adjacent Salt Wash Syncline to the northeast, forming a rim syncline and subjecting the overlying strata to flexure, extension, and fracturing.

Figure 6A: Fracture domain A. Aerial photograph illustrating that fractures in the Entrada Sandstone of fracture domain A are parallel to the axis of the fold. View is to the northwest, along the northeastern limb of the anticline. Individual members of the Entrada Formation are identified by color with the dark red sandstone as the Slick Rock Member and the overlying light-gray to white sandstone as the Moab Member. Figure 6B illustrates how arching of strata over a rising salt core causes extensional fracturing parallel to the axis of the arch.

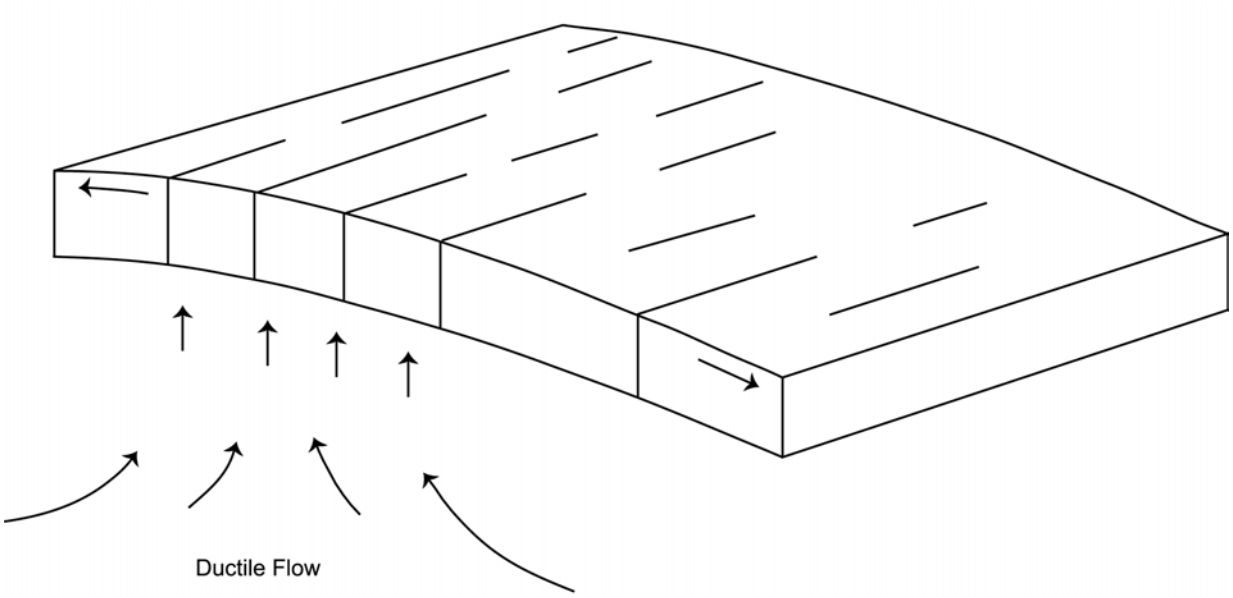

Figure 6B: Fracture domain A. Diagrammatic illustration of how ductile flow of a rising salt core bends the overlying strata forming extension fractures striking parallel to the axis of the arching strata.

2.2.2 Fracture Domain B

The flank of the Salt Valley Anticline flattens to a more gentle dip southeast of domain A, and its strike gradually changes clockwise by 10-12^{o}. Concurrently, the fracture strikes in domain B begin to fan out, those farthest from the crest of the Salt Valley Anticline changing strike counterclockwise by 15-20^{o} (Figures 5, 7A,B), those closer to the crest showing very little change in strike. The fractures locally strike up to 30^{o}–40^{o} oblique to the present bedding strike.

This is a significant change in the relationship between fracture strike and structure from the primitive pattern seen in domain A, and it derives from the subtly compound structural history of the strata. As discussed below, the structure and fracture patterns suggest that the southern part of the Salt Valley Anticline probably initiated as a separate structure, offset slightly to the southwest of the axis of the main structure, and that the two anticlines coalesced during the formation of the present structure.

A fanning fracture pattern is interpreted to be associated with fan-wise extension normal to the axis of a plunging anticline (Figure 7B) or to fan-wise extension at the nose of a syncline. From observations at Palm Valley Anticline, in Australia, Berry et al. (1996) describes a different dominant fracture pattern within the plunging nose region of an anticline. They suggest fractures would radiate or splay away from the anticlinal axis due to the downward bending of the fold axis. Alternatively, Cooper (2000) and Cooper et al. (2001) describe fractures at Teapot Dome, in Wyoming wherein the dominant fractures are modeled as forming due to extension normal to the axis of the anticline. Within this regime a fanning fracture pattern like that observed at the Salt Valley Anticline would be expected to develop in the plunging nose region of the anticline.

Figure 7A: Fracture domain B. Aerial photograph of fractures in domain B southeast of domain A. View is to the northwest, of a section of the northeastern anticlinal limb several km southeast of Figure 6A. Fractures here begin to fan out and strike up to 40^{o} oblique to bedding strike. Figure 7B illustrates how these fractures are due to fan-wise extension normal to the axis of a plunging anticline.

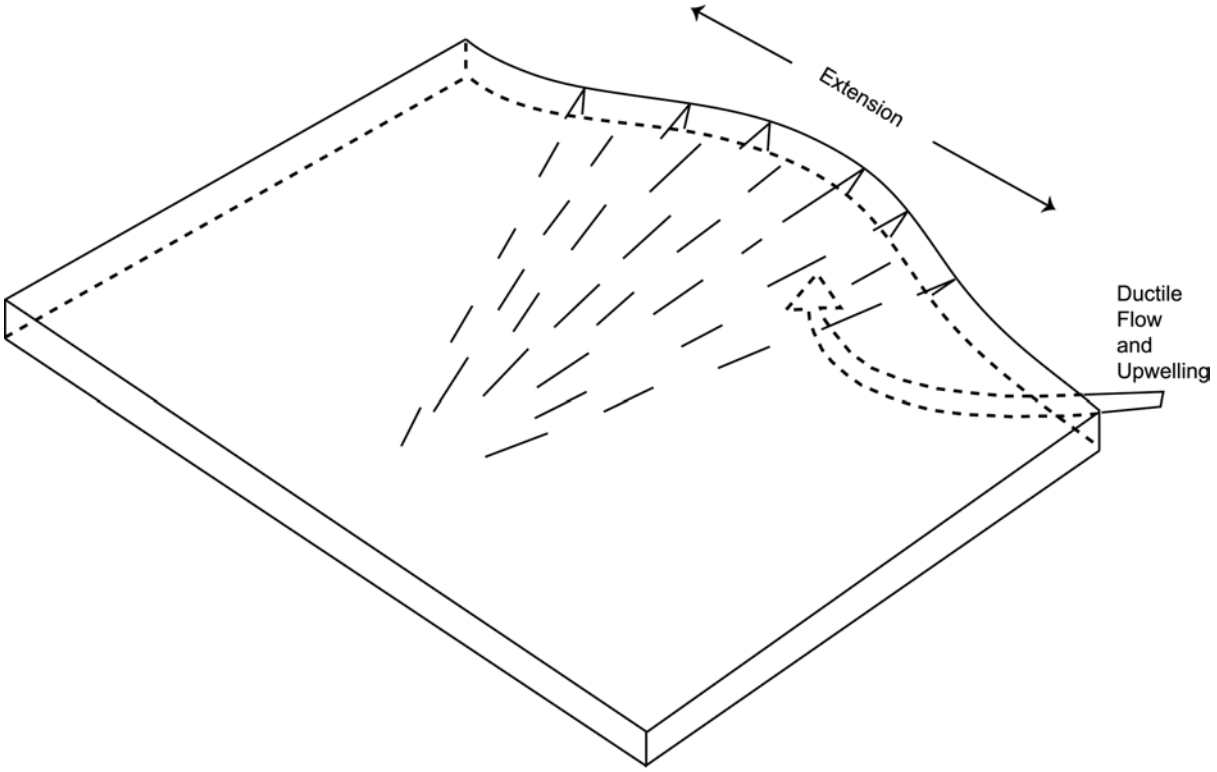

Figure 7B: Fracture domain B. Fracturing due to fan-wise extension normal to the axis of a plunging anticline. Fan-wise extension can also occur near the nose of a syncline. Visualization of fractures associated with a syncline can be achieved by simply turning over the anticline model (above).

The most plausible explanation for the fanning fracture pattern of domain B is that it formed in a local salt-withdrawal depression overlying the source of the adjacent proto-southern anticline. (The Salt Wash Syncline, located just east of the map of Figure 5 and trending sub-parallel to the Salt Valley Anticline, is the larger structure forming the salt-source rim syncline). Remnants of overlying stratigraphic layers disrupt the topography-structure relationship and obscure fracture patterns in this area, but fractures seem to form radiating patterns at the northwest and southeast of the local depression, as would be expected of extension at the noses of a broad syncline.

2.2.3 Fracture Domain C

The fractures in domain C strike nearly parallel to fractures in domain A, and the beds in both zones have strikes that are parallel to the general axis of the anticline (Figure 5). However, the topography/structure-contours show that the transition zone between domains B and C is structurally oblique to the overall axis of the anticline, forming a shallow-angle dog-leg within the flank of the anticline. This transition zone contains an intriguing pattern of overlapping fractures (Figure 8). The structural and fracture geometries suggest the following progression in fracture propagation (Figure 9):

1. Two, semi-simultaneously active, axially-offset, salt-cored anticlines were initially located approximately adjacent to (southwest of) domains A and C.
2. Fractures in domain B formed at the northwest corner of a broad depression, salt from beneath this depression fed evaporites to the anticline adjacent to domain C as described above.
3. Fractures from domain A propagated southward as the salt-cored anticline rose, and fanned out into domain B as salt was withdrawn from underneath the area immediately to the southeast. Fractures from domain C propagated northward as that precursor anticline rose.
4. Propagating fractures from each domain changed their direction of propagation as they entered the adjacent regions of differently oriented stresses between the two anticlines.
5. As the two precursor anticlines coalesced, continued uplift of the flanks of the now-composite anticline warped the strata within this dog-leg in new directions, superimposing new, low-angle-oblique fracture orientations onto the existing fractures.

Figure 8: Fracture Domain C. The transition zone between fracture domains B and C is oblique to the general axis of the anticline and is an area of overlapping fractures. View is to the northwest.

A) Fracturing of domain B; inactive domain C

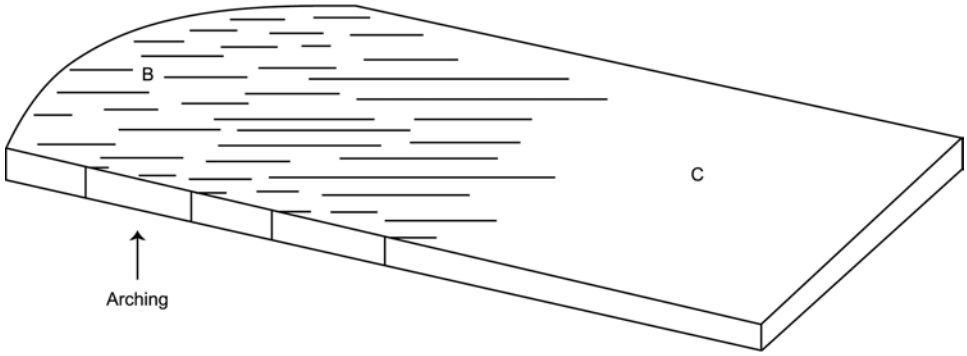

B) Domain B becomes inactive, domain C activity begins. Fractures from domain B propagate into domain C along new anticlinal axis.

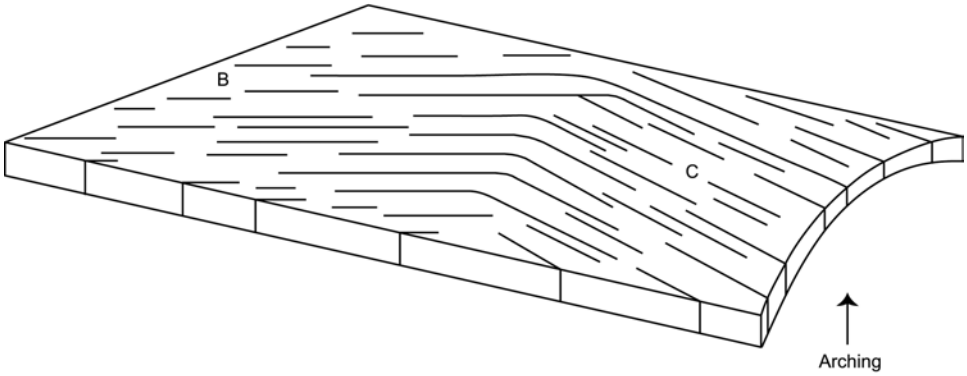

C) Domain C activity and axis of fracturing extends back into domain B, creating oblique cross fractures.

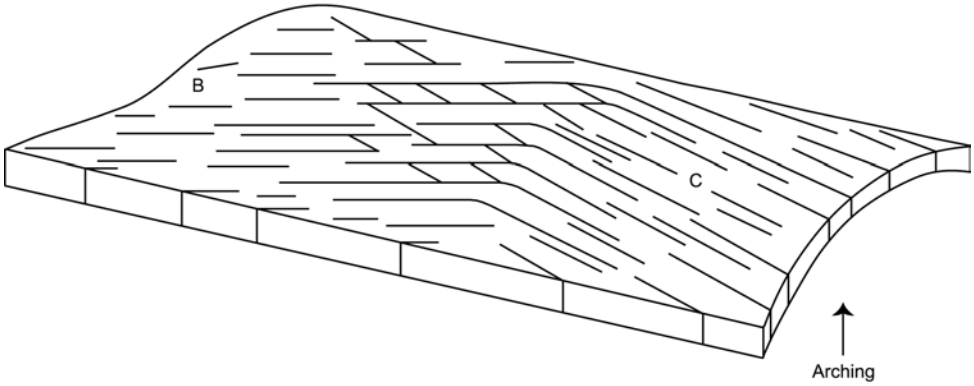

Figure 9: Fracture Domain C. Sequence of fracture development that could produce the observed transition zone between, as well as orientation of fracture domains B and C. Arching at two different times is inferred: A) fractures of domain B form as the older set; B) fractures in domain C propagate next, some of which initiate from pre-existing domain B fractures; C) others form oblique cross fractures within domain B.

2.2.4 Fracture Domain D

Domain D is composed of several fracture sub-domains on a small, east-west trending, anticlinal nose (Figure 5). This nose forms an anomalous, oblique appendage at the southern end of the Salt Valley Anticline, owing its existence to an east-west fault system that marks the southeastern end of the anticline. High-altitude photos suggest that both the structure and the fracture patterns of domain D transition gradually but definitively from domain C. However, oblique, low-altitude photographs (Figure 10A) show that the fracture pattern transitions rather abruptly between the two domains, with a distinct change in fracture frequency and a seven-degree change in structural strike at an ill-defined line. The associated abrupt decrease in spacing suggests an increase in strain, consistent with the tighter structure of the nose. The mutually abutting nature of the fracture intersections at the transition between domains C and D suggests that the fractures formed synchronously, propagating towards each other.

The primary fractures of domain D (those that are contiguous with the fractures of domain C) fan out westward from the eastward-plunging axis of the nose to form region D_1. This fracture pattern and its relationship to structure are similar to those inferred for fracture radiation about the axis of a developing synclinal nose in domain B, only the sense of curvature is inverted. The origin of the fractures is thus inferred to be similar, i.e., fractures formed normal to the direction of extension on the anticline, with the direction of extension changing with strike of the beds on the plunging nose.

Domain D_2 (Figure 10B) consists of an enigmatic superposition of what appear to be conjugate shear fractures onto the D_2 fracture system. If these are in fact conjugate fractures, they imply a unique, local zone of compression for which a ready explanation is not apparent within this overall extensile setting. However, a wide gulch marks the eastern crest of the nose, suggesting extension faulting (the gulch is too deep and wide for the non-existent catchment area at the crest of the anticline and thus a primary origin from erosion is unlikely). The absence of this fault in the zone of apparent conjugate fracturing is consistent with compression at the western end of the nose. Such large-scale conjugate shear fracture pairs suggest volume constraints associated with rotation of the strata about a vertical axis (Figure 11). Right-lateral strike-slip along the fault that forms the southern boundary of Domain E (see below) would have enhanced the effect, although lateral slip on this fault has not been mapped.

Figure 10A: Fracture domain D. Aerial photograph illustrating the abrupt transition of fractures from domain C to domain D. View is to the northwest.

Figure 10B: Fracture domain D. Photograph showing the plan view orientation of possible conjugate shear fractures within domain D_2. View is to the southeast.

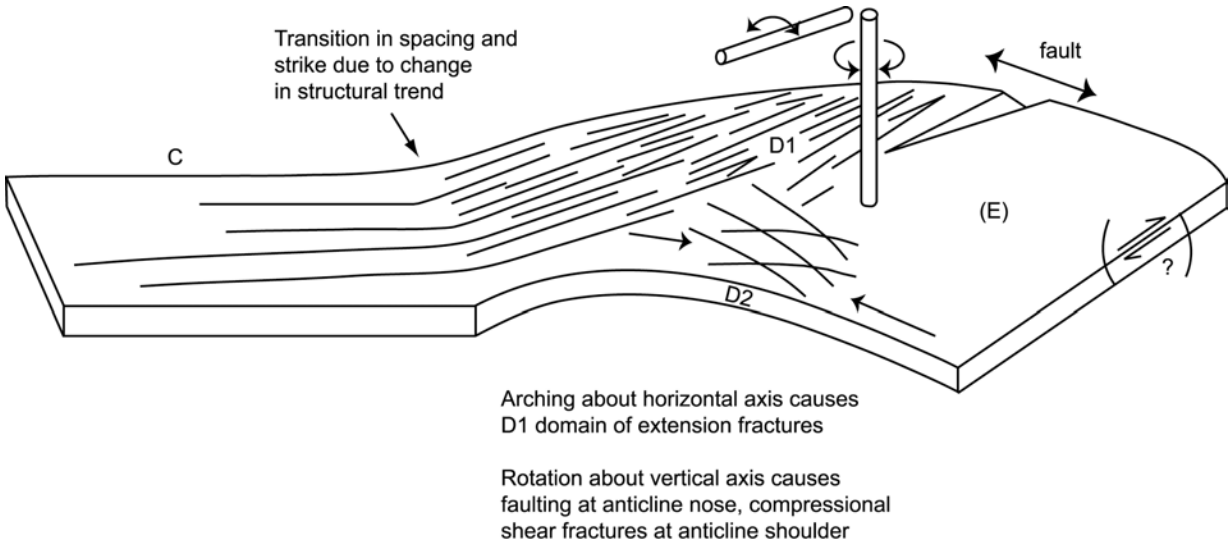

Figure 11: Fracture domain D. Arching about a horizontal axis forms extension fractures of domain D_1. Rotation about a vertical axis causes faulting at the anticlinal nose and compression related shear fractures of domain D_2 at anticline shoulder.

2.2.5 Fracture Domain E

Domain E (Figure 5) contains two superimposed fracture sets (Figures 12, 13, and 14). One set is the southern continuation of the D_1 fracture domain, related to the bending stresses associated with the anticlinal nose and radiating across the domain to maintain a parallel relationship to the structure contours and to the local axes extension on the flexure. The other fracture set trends parallel to both the axial gulch immediately to the north and to the mapped normal fault system that defines the southern edge of the anticline. These fractures are inferred to be an extensional set related to the local faulting.

2.2.6 Fracture Domain F

The compound structural history of the Salt Valley Anticline obscures the fracture-structure relationship northwest of the primitive domain of structure-parallel fractures (domain A), apparently due to a northwestward elongation of the anticline during growth and to the presence of a fault system on the opposite limb in this northern part of the anticline where it narrows. Fractures in domain F transition northwestward out of domain A at the point where fractures start diverging from parallel to become oblique to the strike of local bedding (Figure 5). Both bedding and fracture strikes rotate counterclockwise as traced to the northwest, but fracture strike changes more rapidly, diverging by up to 40^{o} from the strike of bedding.

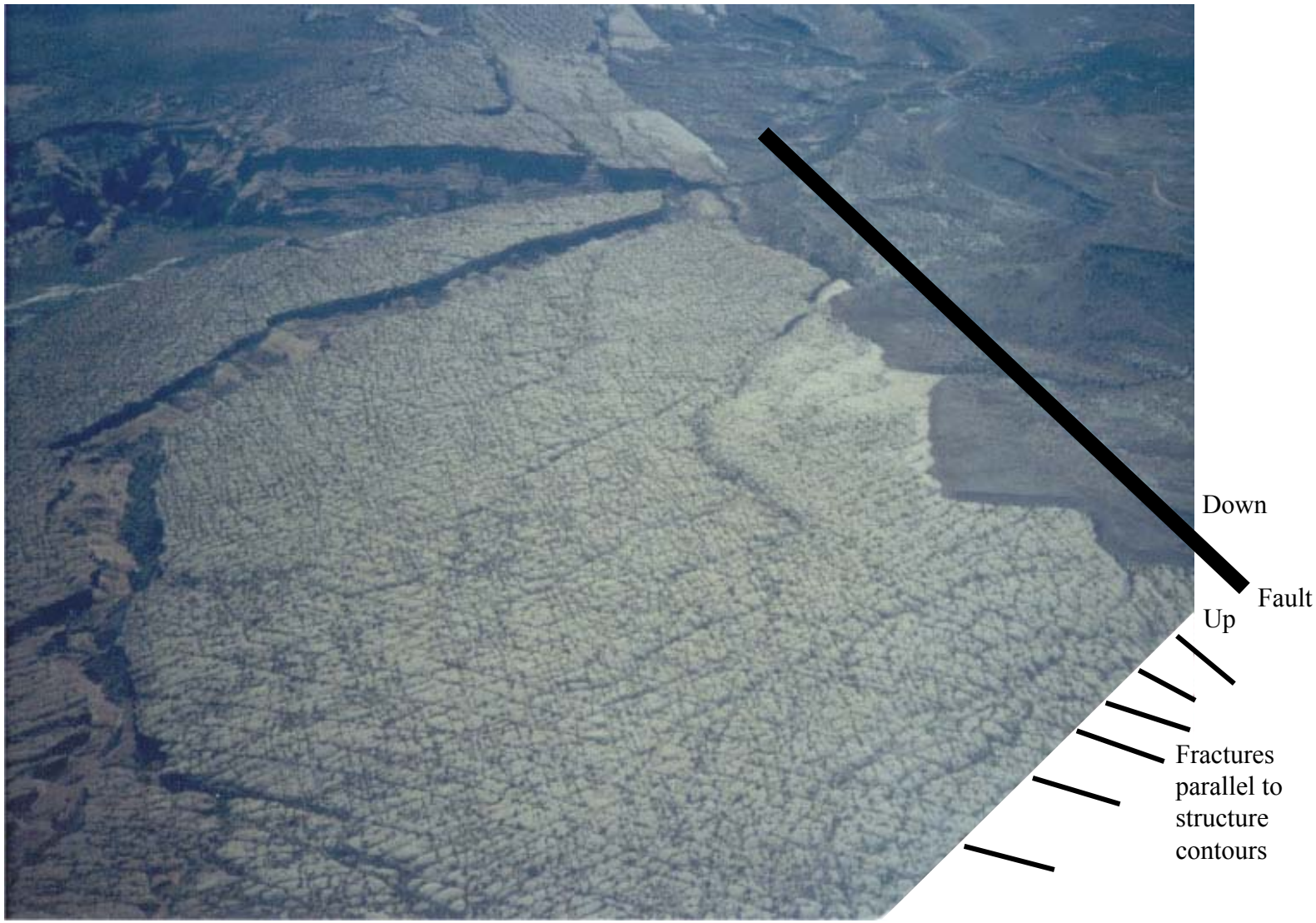

Figure 12: Fracture domain E. Aerial photograph of two fracture sets within domain E. One fracture set is parallel to structure contours the second is parallel to local faulting. View is to the east.

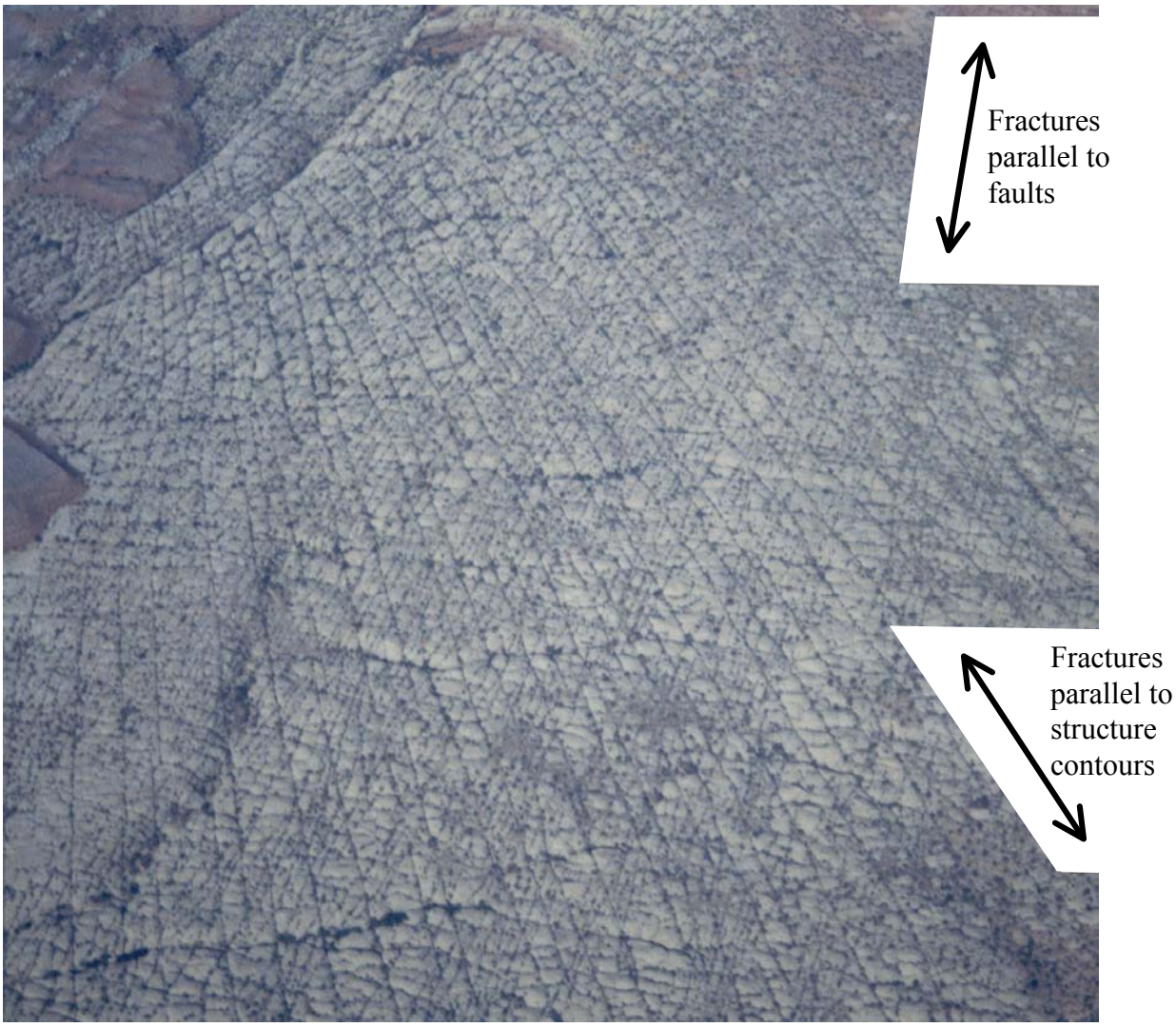

Figure 13: Fracture domain E. Aerial photograph of two fracture sets within domain E. One fracture set is parallel to structure contours the second is parallel to local faulting.

This curvature of fractures suggests that they formed around an early offset in the anticline or an en echelon offset of two incipient anticlines prior to coalescence (much as the transition between domains B and C described above). Continued growth into the present structural configuration "straightened out" the bedding but left a fracture-pattern record of the earlier dogleg. Faults in this area have an intermediate strike between that of the fractures and that of the present structure. Thus the fractures record the early strains associated with early deformation, faults record the continued accumulation of strain but with a slightly different orientation due to the modification of the anticline geometry during growth, and the structure contours represent the present-day configuration.

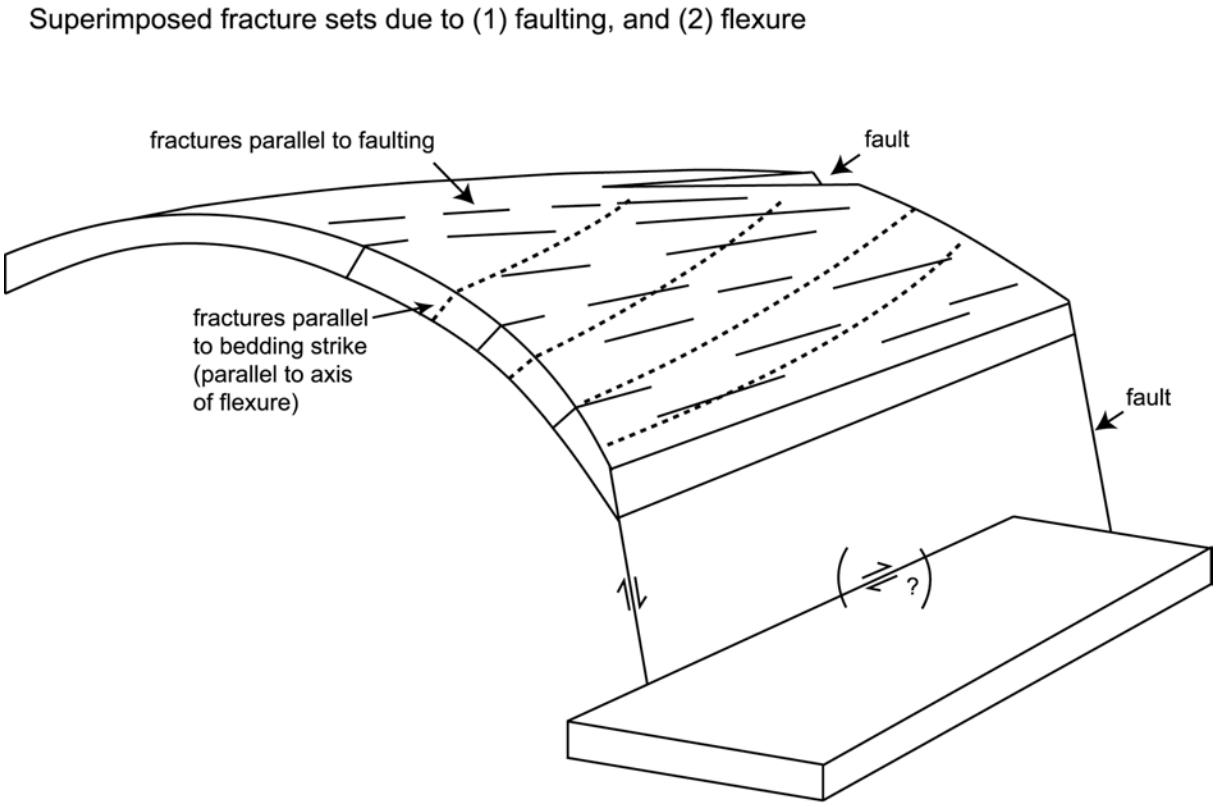

Figure 14: Fracture domain E. Diagrammatic illustration of the relationship between the two fracture sets and (1) local faulting and (2) the axis of flexure.

The relationship between fractures and structure is also complicated by the mechanical stratigraphy of the local formations (it may be equally complex elsewhere on the Salt Valley structure, e.g., the southern end west of domain D, but it is best exposed here). Fracture strikes are not consistent throughout the stratigraphic column in domain E. In fact, there is a 30-40^{o} difference between the structure-oblique strikes of the fractures in the Moab Member just described and the strikes of fractures in the directly underlying Slickrock Member, which more closely parallel the present structure contours (Figure 15).

This indicates that the mechanical rock properties of these two members of the Entrada Formation were sufficiently different that they fractured at different times even though they were subjected to the same composite stress history. The Moab Member fractured early, as described, whereas the Slickrock Member did not fracture until a larger strain had accumulated, whereupon the fracture strikes were more nearly parallel to the present structure (Figure 16). Cruikshank and Aydin (1995) have described a similar relationship, with younger fractures in the Slickrock Member on the southeastern limb of the anticline, and Lorenz (1997) has described and interpreted similar conditions and results in the Wasatch Formation of northwestern Colorado.

Figure 15: Fracture domain F. Aerial photograph of fractures within domain F. There is a distinct $30^{o} – 40^{o}$ variation in fracture strike between the Moab Member and the underlying Slickrock Member of the Entrada Sandstone. View is to the southeast.

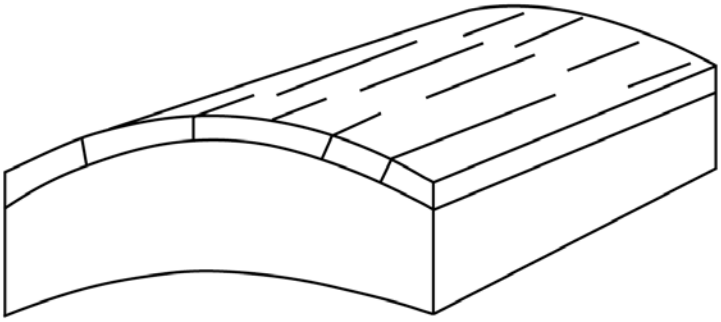

A) Fractures form first in the Moab Member

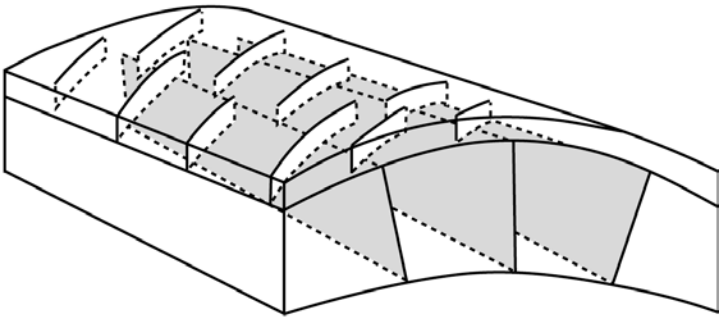

B) Axis of flexure changes:
- New fractures form in the Slickrock Member
- Fractures in Moab Member are reactivated

Figure 16: Fracture domain F. Inferred history for the formation of fractures of two different ages and orientations within adjacent beds. Fractures first form in the overlying Moab Member. Over time the axis of the flexure changes and new fractures form within in the Slickrock Member. Additionally the preexisting fractures within the Moab Member are reactivated.

2.2.7 Fracture Domain G

Domain G (Figure 5) contains two, mutually cross-cutting sets of fractures. The inferred older set is a continuation of Moab-Member fractures from domain E. This set is probably related to the localized precursor anticline. The other fractures are unrelated and cross the first set at nearly right angles. The two sets of fractures are equally well developed. The origin of the stresses that caused the second set of fractures is not apparent.

2.2.8 Fracture Domain H

Numerous fracture sets are present on the southwestern limb of the Salt Valley Anticline, but their relationship to the structure is not as clear-cut as those described above and they were not investigated here. In part, this may be due to the complicating presence of a fault system paralleling this limb of the anticline and that is probably related to dissolution and collapse along the crest of the structure. However, there is a region 'domain H' outside the mapped area of Figure 5 that again appears to be a definable relationship between fracturing and structure. This is the Courthouse syncline, a broad depression located southeast of and parallel to the Salt Valley anticline. Hudec and May (1998, 1999) have suggested that this area was the locus of salt accumulation (the "Courthouse salt wall") during Permian time, but that this structural high collapsed and became the locus of northwestward-prograding sedimentation from late Permian through Cretaceous time. Extension normal to the axis of the syncline, either during its anticlinal or synclinal phase, produced a systematic set of distinctive, axis-parallel, relatively short fractures within the surface strata exposed along the present Courthouse syncline (Figure 17).

2.3 Applicability: Salt Valley Anticline Fractures as an Analog to Reservoirs in the Cane Creek Shale

Oil is produced from the Cane Creek Shale interval of the Paradox Formation at six fields within the Paradox Basin. This interval is composed of highly fractured dolomitic siltstone and shale interbedded with halite and other evaporites (Morgan and Chidsey, 1991; Grove and Rawlins, 1997). Morgan and Chidsey (1991) indicate that fracture orientation is related to folding, with the more productive fractures occurring along the crest and flanks of anticlinal structures. Grove and Rawlins (1997) note that these highly permeable fracture systems also have a complex history that is related to episodic movement of salt within the Paradox Formation. Thus the fractures within the Cane Creek Shale interval are probably similar in initiation and propagation history to those observed within the Entrada Formation at Arches National Park. That is, the fractures are formed during salt flowage and the formation of anticlines and synclines. As observed at Arches National Park these structures have a complex history. Therefore, the fracture patterns on the surface at Arches provide a direct model for the subsurface Cane Creek interval. This in turn may help determine the best orientation for horizontal drilling to intersect the maximum number of these fracture systems.

Figure 17: Aerial photograph of the Courthouse Syncline. Fractures within this broad syncline are parallel to the axis of the syncline. The fractures probably resulted from extension normal to the axis during subsidence driven by withdrawal of underlying evaporites.

3.0 HOLBROOK ANTICLINE, EASTERN ARIZONA

The Holbrook anticline is located along the southern margin of the Holbrook basin in east central Arizona (Figure 18). Like the Salt Valley structure this anticline is cored by Paleozoic evaporites. Overlying strata at the Holbrook anticline were passively folded over a salt-dissolution front (Neal and Lorenz, 1988). Thus the Holbrook structure is similar to an early stage in the development of the Salt Valley anticline wherein the anticline is not substantially breached however folding, fracturing and fracture modification has occurred.

The Coconino and related sandstones in the Holbrook basin overlie the Corduroy Member of the Schnebly Hill Formation, a thick (1000 ft) evaporitic sequence of halites, shales, and anhydrites. Although regional dip into the basin is only 1-2 degrees to the north, the Coconino Sandstone contains both prominent regional fractures, and due to mobility of the underlying salt, locally superimposed irregular fractures. Fractures are especially evident over the Holbrook anticline where dissolution of the underlying evaporites has reversed bedding dips to a 10-degree southerly dip and widened the regional fractures at the surface (Figure 18; Lorenz and Neal, 1997; Neal and Lorenz, 1998).

Sinkholes are evident at the Holbrook anticline (Figures 18 and 19) but are not observed at Salt Valley. This is primarily due to the breached and more eroded (mature) nature of the Salt Valley anticline. Regional fractures along the crest and limbs of the Holbrook anticline are being extended into fissures and in places are vertically offset due to salt dissolution (Figures 20A, B and 21).

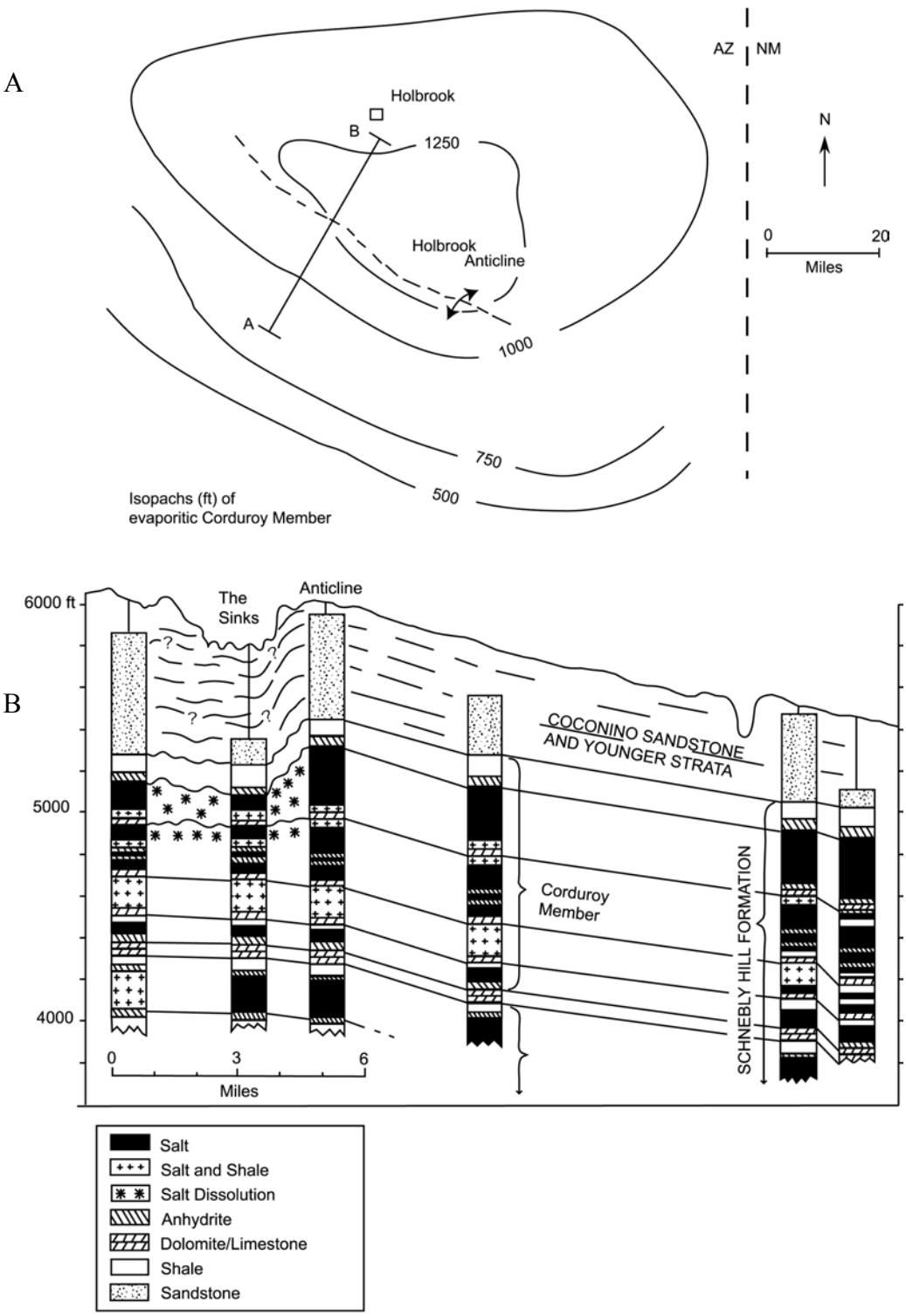

Figure 18: A) Isopach map of the evaporitic Corduroy Member of the Schnelby Hill Formation in the Holbrook Basin of northeastern Arizona. B) Cross-section line A-B illustrating the dissolution front along the southwestern edge of the Holbrook Anticline.

Figure 19: "The Sinks": sink holes in the Coconino Sandstone along the crest of the Holbrook Anticline highlight the presence and instability of the underlying evaporites. Sinks are superimposed onto a sub-parallel fracture pattern, trending upper left to lower right.

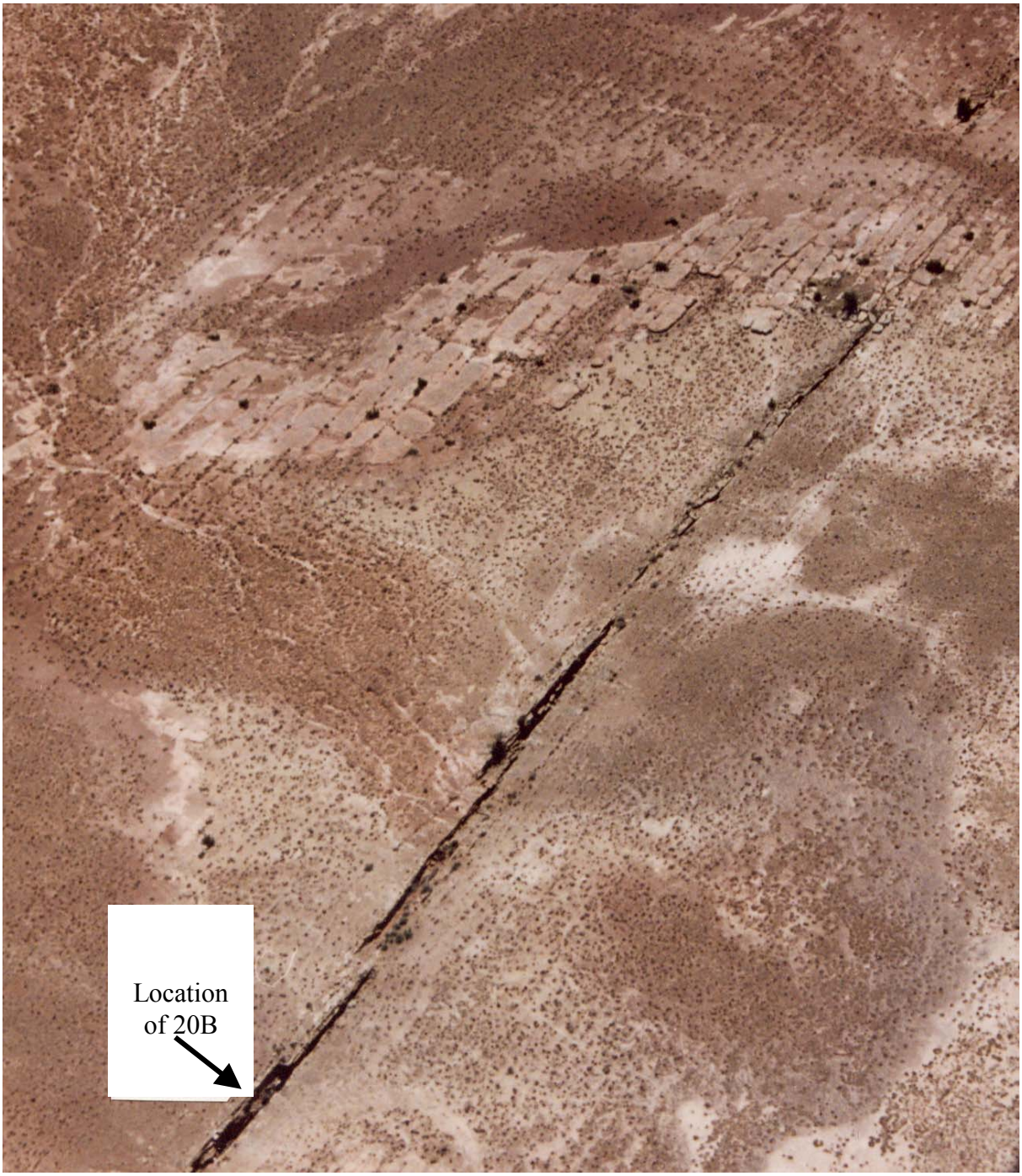

Figure 20A: A single set of regional fractures on the Moenkopi and Kaibab formations (overlying the Coconino Sandstone) near the crest of the Holbrook Anticline is being extended into local fissures by dissolution and related mobility of the evaporites.

Figure 20B: Close-up photograph of location designated in Figure 20A. The natural fissure has been used as a dump site.

Figure 21: Aerial photograph of the Twin Lakes area on the southern limb of the Holbrook Anticline. Here the fractures are being widened and offset vertically by dissolution of the underlying strata.

4.0 FRONTIER FORMATION, HOGSBACK THRUST PLATE, SOUTHWESTERN WYOMING

Fracture development in sandstones due to ductile deformation of shales can be similar to fracture development associated with salt mobility such as the Salt Valley anticline. Fractures within sandstones of the Frontier Formation along Oyster Ridge in southwestern Wyoming are related to an underlying thin-skinned thrust and the contemporaneous ductile deformation of shale interbeds.

The Oyster Ridge Sandstone Member of the Frontier Formation outcrops along a 60-mile long ridge (Oyster Ridge). The ridge was formed by uplift along the underlying Hogsback thrust of the Idaho-Wyoming Thrust Belt. The Oyster Ridge Sandstone Member is 20 meters thick and is interbedded within thick (a few hundreds of meters) units of the Hilliard and Steele shales. Oyster Ridge sandstones are ubiquitously fractured, the fracture patterns varying significantly as a function of structural location (Figures 22 and 23).

Ductile deformation of the thick shales that enclose the Oyster Ridge Sandstone allowed kilometer-scale lateral offsets to form in the thrust sheet without creating major tear faults. However, this offset strain was recorded within the relatively thin and brittle sandstone sheets by the formation of additional oblique fracture sets, superimposed on the relatively uniform pre-existing fractures (Figures 24 and 25; Lorenz and Laubach, 1994).

Fractures along Oyster Ridge, similar to fractures found in structurally simple settings at Salt Valley, have orientations that are nearly parallel and normal to the strike of bedding. More structurally complex areas show changes in fracture strike due to a change in strike of the underlying thrust (Figure 24) or a younger fracture set superimposed on an older set (Figure 25) due to local structural complications.

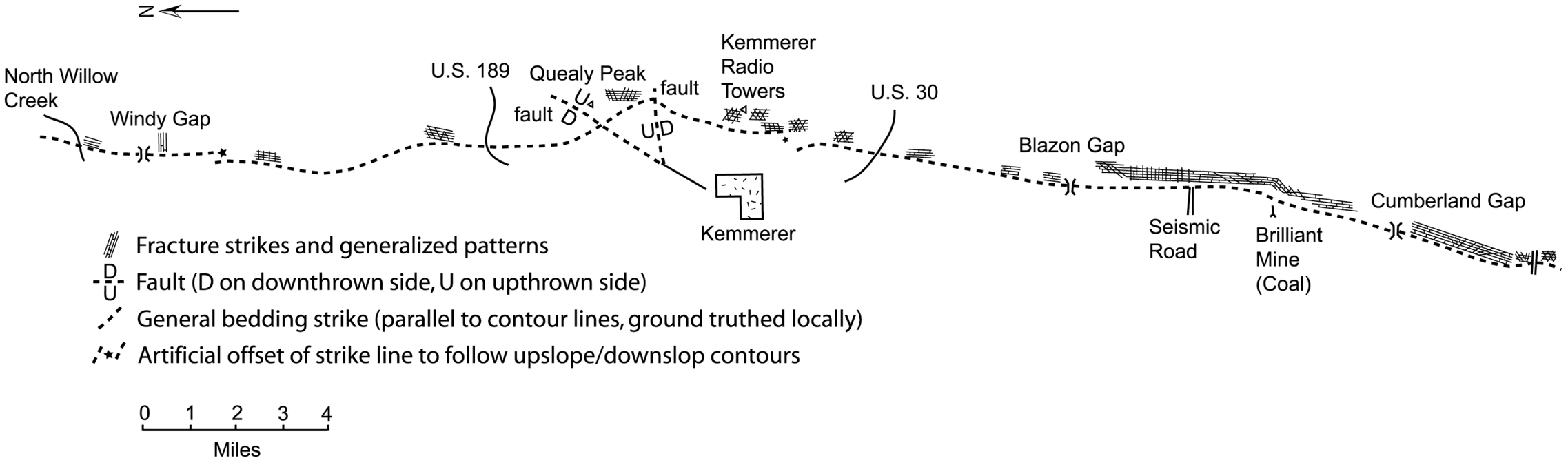

Figure 22: Structural trends and generalized fracture patterns along the Hogsback Thrust/Oyster Ridge. The bends in the thrust plate at Quealy Peak and the Kemmerer radio towers have caused significant perturbations in the strike-parallel and strike-normal fracture patterns (modified from Lorenz and Laubach, 1994).

Figure 23: Aerial photograph illustrating the fracture pattern on a bedding-plane surface in a structurally simple area near the seismic road in Figure 22, wherein the oldest fractures are strike-parallel (horizontal across the photograph) and younger fractures are strike-normal (vertical across the photograph). View is to the east.

Figure 24: Low-angle aerial photo of the change in strike of the thrust fault due to local lateral offset at the Kemmerer radio towers. View is to the southeast from just north of Kemmerer. Bedding plane surface of the Oyster Ridge Sandstone Member of the Frontier Formation

Figure 25: Oblique fracture patterns superimposed onto strike-parallel and strike-normal fractures in the Kemmerer area (from the area indicated by the arrow in Figure 24). Two-track road across middle of photo for scale. Fractures pavement is a bedding plane surface of the Oyster Ridge Sandstone Member of the Frontier Formation.

5.0 CONCLUSIONS

Sandstones overlying or interbedded with ductile strata commonly contain different fracture domains. Each domain contains a specific fracture pattern and can cover an area of a few square miles. The fracture pattern within a domain is related to stresses arising from flexures that are in turn a result of the mobility and/or dissolution of ductile strata. Superimposed fracture sets can occur within a domain and are the result of episodic movement of ductile strata and the resulting compound geologic history.

Given the inherent complexities of fracture development under this regime it is difficult to predict subsurface fracture patterns. Nevertheless numerous clastic reservoirs are found within areas influenced by movement or dissolution of ductile strata. Therefore, outcrop observations and characterization at Arches National Park and similar structures are an important step in understanding fracture patterns and fracture domains within subsurface reservoir rocks.

6.0 ACKNOWLEDGMENTS

This work was sponsored by the National Petroleum Technology Office of the National Energy Technology Laboratory (US Department of Energy), Tulsa, OK. Our thanks to Bob Lemmon, contract manager, for supporting this project. Sandia is a multiprogram laboratory operated by Sandia Corporation, a Lockheed Martin Company, for the United States Department of Energy under contract DE-AC04-94AL85000.

7.0 REFERENCES

Berry, M. D., Stearns, D. W., and Friedman, M., 1996, The development of a fractured reservoir model for the Palm Valley gas field: Australian Petroleum Production and Exploration Association Journal, v. 36, no. 1, p. 82-103.

Cooper, S. P., 2000, Deformation within a basement-cored anticline Teapot Dome, Wyoming [M.S. thesis]: New Mexico Institute of Mining and Technology, 274 p.

Cooper, S. P., Lorenz, J. C., and Goodwin, L. B., 2001, Lithologic and Structural Controls on Natural Fracture Characteristics Teapot Dome, Wyoming, Sandia National Laboratories Technical Report, Sand2001-1786, p. 73.

Cruikshank, K. M., and Aydin, A., 1994, Role of fracture localization in arch formation, Arches National Park, Utah: Geological Society of America Bulletin, v. 106, p. 879-891.

Cruikshank, K. M., and Aydin, A., 1995, Unweaving the joints in Entrada Sandstone, Arches National Park, Utah, U.S.A.: Journal of Structural Geology, v. 17, p. 409-421.

Doelling, H. H., 1985, Geologic map of Arches National Park and vicinity, Grand County, Utah: Utah Geological and Mineral Survey Map 74.

Doelling, H. H., 1988, Geology of Salt Valley Anticline and Arches National Park, Grand County, Utah, *in* Doelling, H. H., Oviatt, C. G., and Huntoon, P. W., eds., Salt Deformation in the Paradox Basin: Utah Department of Natural Resources Bulletin 122, p. 1-58.

Doelling, H. H., 2000, Geology of Arches National Park, Grand County, Utah, *in* Sprinkel, D. A., Chidsey, T. C., and Anderson, P. B., eds., Geology of Utah's Parks and Monuments, Utah Geological Association Publication 28, p. 11-36.

Dyer, J. R., 1983, Jointing in Sandstones, Arches National Park, Utah [Ph.D. Dissertation]: Stanford University, 202 p.

Dyer, R., 1988, Using joint interactions to estimate paleostress ratios: Journal of Structural Geology, v. 10, no. 7, p. 685-699.

Grove, K. W., and Rawlins, D. M., 1997, Horizontal exploitation of oil and gas-bearing natural fracture systems in the Cane Creek Clastic interval of the Pennsylvanian Paradox Formation, Grand and San Juan Counties, Utah, *in* Close, J. C., and Casey, T. A., eds., Natural Fracture systems in the Southern Rockies: Four Corners Geological Society Guidebook, p. 133-134.

Hite, R. J., 1977, Subsurface geology of a potential waste emplacement site, Salt Valley anticline, Grand County, Utah, United States Geological Survey Open-file Report 77-761, p. 26.

Hudec, M. R., and May, S.R., 1998, The Courthouse Syncline; A Gulf of Mexico-style minibasin exposed in the Paradox Basin, Utah: American Association of Petroleum Geologists Annual Meeting Extended Abstracts on CD, not consecutively numbered.

Hudec, M. R., and May, S. R., 1999, Control of sediment progradation on salt geometry, and vice-versa, in the northeastern Paradox Basin, Utah: American Association of Petroleum Geologists and Society of Economic Paleontologists and Mineralogists Annual Meeting Abstracts, p. A64.

Lorenz, J. C., 1997, Heartburn in predicting natural fractures: The effects of differential fracture susceptibility in heterogeneous lithologies, *in* Hoak, T. E., Klawitter, A. L., and

Blomquist, P. K., eds., Fractured reservoirs: Characterization and modeling: Rocky Mountain Association of Geologists Guidebook, p. 57-66.

Lorenz, J. C., and Laubach, S. E., 1994, Description and interpretation of natural fracture patterns in sandstones of the Frontier Formation along the Hogsback, southwestern Wyoming: Gas Research Institute, Tight Sands and Gas Processing Research Department, GRI-94/0020, p. 89.

Lorenz, J. C., and Neal, J. T., 1997, Fractured reservoirs in sandstones interbedded with evaporites: Good news and bad news: Annual Meeting Abstracts - American Association of Petroleum Geologists and Society of Economic Paleontologists and Mineralogists, p. 72.

Morgan, C. D., and Chidsey, T. C., 1991, Horizontal drilling potential of the Cane Creek Shale, Paradox Formation, Utah: American Association of Petroleum Geologists Bulletin, v. 75, no. 6, p. 1133-1134.

Neal, J. T., and Lorenz, J. C., 1998, Holbrook Anticline, Arizona: An exposed analog for fractured reservoirs over salt-dissolution fronts, SPE paper number 49027, SPE Annual Technical Conference and Exhibition, New Orleans, Louisiana.

Oviatt, C. G., 1988, Evidence for Quaternary deformation in the Salt Valley anticline, southeastern Utah, *in* Doelling, H. H., Oviatt, C. G., and Huntoon, P. W., eds., Salt Deformation in the Paradox Basin: Utah Department of Natural Resources Bulletin 122, p. 61-78.

Zhao, G., and Johnson, A. M., 1991, Sequential and incremental formation of conjugate sets of faults: Journal of Structural Geology, v. 13, p. 887-895.

Zhao, G., and Johnson, A. M., 1992, Sequence of deformations recorded in joints and faults, Arches National Park, Utah: Journal of Structural Geology, v. 14, p. 225-236.

Distribution

Paul Basinski
El Paso Production
Four Greenway Plaza
Houston, TX 77046

Randal L. Billingsley
4 Wild Turkey Lane
Littleton, CO 80127
(303) 979-3559

Burlington Resources
PO Box 4289
Farmington, NM 87499-4289
Chip Head
Michael Dawson

Jock A. Campbell
Oklahoma Geological Survey
University of Oklahoma
Sarkeys Energy Center
100 E. Boyd Street, Room N-131
Norman, Oklahoma 73019-0628

David B. Codding
Yates Petroleum Corporation
105 South Fourth Street
Artesia, NM 88210

Dan M. Cox
Veritas DGC Inc.
Exploration Services Division
10300 Town Park
Houston, TX77072

Murray Dahill
523 S. Park
Casper, WY 82601

New Mexico Institute of Mining and Technology
Department of Petroleum Engineering
Socorro, NM 87801
Larry Teufel

Tom Engler
Geospectrum, Inc.
214 W. Texas
Suite 1000
Midland, TX 79701
James J. Reeves
W. Hoxie Smith

Leo A. Giangiacomo
Extreme Petroleum Technology, Inc.
2033 Begonia St.
Casper, WY 82604

Catherine Hanks
Geophysical Institute
University of Alaska
Fairbanks, AK 99775

Hugo Harstad
Norsk Hydro
EPI-New Ventures
KJ 8.2
0246 Oslo, Norway

Bruce Hart
Earth and Planetary Sciences
McGill University
3450 University Street
Montreal, QC
CANADA H3A 2A7

Ralph L. Hawks, Jr.
Williams Energy
PO Box 3102
Tulsa, OK 74101

Peter H. Hennings
Geoscience Branch
Upstream Technology and Project Development
Phillips Petroleum Company
510 A Plaza Office Building
Bartlesville, OK 74004

Stephan A. Hines
Navajo Nation Oil and Gas Co. Inc.
P.O. Box 4439
Window Rock, AR 86515

James M. Hornbeck
Hornbeck Geological Consulting
5101 College Boulevard
Farmington, NM 87402-4709

Neil F. Hurley
Department of Geology and Geological Engineering
Colorado School of Mines
Golden, CO 80401

Robert Lemmon (10)
National Petroleum Technology Office
One West Third Street
Tulsa, OK 74103-3519

Alvis L. Lisenbee
Geology and Geological Engineering Department
South Dakota School of Mines and Technology
501 E. St. Joseph
Rapid City, SD 57701

Marathon Oil Co
100 West Missouri St
Midland, TX 79701
Jim Bucci
Jim Minelli

Tom Mather
Howell Petroleum Corp.
1111 Fannin St., suite 1500
Houston, TX 77002 – 6923

Curt McKinney
Devon Energy Corporation
20 North Broadway, Suite 1500
Oklahoma City, OK 73102-8260

Mark Milliken
Rocky Mountain Oilfield Testing Center
907 N. Poplar
Suite 150
Casper, WY 82601

Jim Murphy
Conoco, Inc
600 North Dairy Ashford
Houston, TX 77079-1175

National Energy Technology Laboratories
PO Box 880
Morgantown, WV 26507-0880
Thomas Mroz (10)
James Ammer
Gary Covatch
Mark McKoy

Ronald A. Nelson
BP Amoco
501 Westlake Park Blvd.
Houston, TX 77079-2696

New Mexico Institute of Mining and Technology
Department of Earth and Environmental Science
801 Leroy Place
Socorro, NM 87801
Laurel B. Goodwin
Peter S. Mozley
Steve Ralser

New Mexico Bureau of Mines and Mineral Resources
New Mexico Institute of Mining and Technology
801 Leroy Place
Socorro, NM 87801-4796
Steven M. Cather
Ron Broadhead
Brian Brister

Joseph Piombino
BP Amoco Exploration
P.O. Box 3092

501 WestLake Park Boulevard
Houston, TX 77079-2696

Charles Schelz (5)
Biologist
National Park Service
2282 SW Resource Blvd
Moab, Utah 84532

Mr. Harry L. Siebert
14780 Highway 145
Dolores, CO 81323-8200

John D. Taylor
River Gas Corporation
1300 McFarland Blvd. NE
Suite 300
Tscaloosa, AL 35406

Thomas L. Thompson
Thompson's Geo-Discovery, Inc.
580 Euclid Avenue
Boulder, Colorado 80302

Margot Timbel
Director, North American Exploration
ANSCHUTZ Exploration Corporation
555 Seventeenth Street
Suite 2400
Denver, CO 80202

US Geological Survey
Denver, CO 80225
Curt Huffman, MS 939
Steve Condon, MS 939

Jerry Walker
Independent Geologist
1455 Shewmaker Court
Reno, NV 89509

Sandia National Laboratories
Albuquerque, NM 87185
Stephen Bauer, MS 0706
William Olsson, MS 0751
Marianne Walck, MS 0750
Scott Cooper, MS 0750 (30)
John Lorenz, MS 0750 (30)

Central Technical Files, 8945-1, MS 9018
Technical Library, 9616, MS 0899 (2)
Review and Approval Desk, 9612, MS 0612
For DOE/OSTI